

# Experimental Study of the Methodology for the Modelling and Simulation of Mobile Manipulators

Regular Paper

Luis Adrian Zuñiga Aviles<sup>1, 2, \*</sup>, Jesus Carlos Pedraza Ortega<sup>1, 2</sup> and Efren Gorrostieta Hurtado<sup>1, 2</sup>

<sup>1</sup> Secretariat of National Defense and CIDEI, México

<sup>2</sup> CIDIT-Facultad de Informática, Universidad Autónoma de Querétaro, México

\* Corresponding author E-mail: [adrian\\_dgim@prodigy.net.mx](mailto:adrian_dgim@prodigy.net.mx)

Received 7 May 2012; Accepted 27 Jul 2012

DOI: 10.5772/518671

© 2012 Aviles et al. ; licensee InTech. This is an open access article distributed under the terms of the Creative Commons Attribution License (<http://creativecommons.org/licenses/by/3.0/>), which permits unrestricted use, distribution, and reproduction in any medium, provided the original work is properly cited.

**Abstract** This paper describes an experimental study of a novel methodology for the positioning of a multi-articulated wheeled mobile manipulator with 12 degrees of freedom used for handling tasks with explosive devices. The approach is based on an extension of a homogenous transformation graph (HTG), which is adapted to be used in the kinematic modelling of manipulators as well as mobile manipulators. The positioning of a mobile manipulator is desirable when: (1) the manipulation task requires the orientation of the whole system towards the objective; (2) the tracking trajectories are performed upon approaching the explosive device's location on the horizontal and inclined planes; (3) the application requires the manipulation of the explosive device; (4) the system requires the extension of its vertical scope; and (5) the system is required to climb stairs using its front arms. All of the aforementioned desirable features are analysed using the HTG, which establishes the appropriate transformations and interaction parameters of the coupled system. The methodology is tested with simulations and real experiments of the system where the error RMS average of the positioning task is 7.91 mm, which is an acceptable parameter for performance of the mobile manipulator.

**Keywords** Methodology, Modelling, Simulation, Experimental study, Wheeled mobile manipulator, Positioning

## 1. Introduction

Mobile manipulators exhibit wide versatility in the handling of dangerous devices, such as the explosive ordinance devices (EOD) used by the world's armies. Among the most important phases in the mechatronic design of mobile manipulators we have modelling and simulation, because upon them depends the proposed control for its correct operation and the fact that its behaviour will be verified by the simulation of several instances in order to obtain the parameters and ranks from the mobile manipulator that is being developed.

In relation to the modelling of mobile manipulators, the work of Yamamoto, Alicja Mazur and Bayle is well known. Yamamoto is the most cited, with his paper on the locomotion coordination of mobile manipulators, published in 2004. Alicja Mazur and Bayle are the authors that have written most in relation to this topic. Since 1976,

there are records of works related to the programming of teleoperated mobile manipulators [1]; moreover, in 1988 [2] and 1996 [3-4], the dynamics of mobile manipulators in the operational case of the opening of a door was proposed; however, the manipulator and the mobile platform were considered and analysed separately. Besides this, from 1994 to 2008, some works were published on mobile manipulators with planar manipulators but without considering the load or other operational cases; they were focused only on control, kinematic redundancy, tracking trajectories and manipulability [5, 18, 26, 29].

In order to obtain the modelling of mobile manipulators used in the tasks for positioning in the handling and transport of explosive devices, the present work considers the development of a modelling methodology for mobile manipulators by applying the mechatronic design of a multi-articulated wheeled mobile manipulator called Robot MMR12-EOD. Unlike the others methodologies presented in previous works, it considers the problem of the mechatronic design, the coupled full system and kinematic modelling in real operations. An experimental study of the methodology capable of performing this positioning in real operational scenarios is described throughout this paper.

The rest of the paper is organized as follows. Section 2 describes the methodology for the kinematic modelling of the full system and the experiments in several scenarios of operation. Later, section 3 presents the results in which the basis of the reference values that were obtained in the modelling are presented with the errors from the simulation and the real experiment, comparing them with the ideal parameters and both errors. This work is discussed and is concluded in Sections 4 and 5, respectively.

## 2. Modelling and Simulation Methodology

This section presents the modelling methodology for wheeled mobile manipulators, describing the planning, development and experimentation. It is organized as follows: preliminary analysis, master map, diagram of position and orientation, homogenous transformation graph, kinematic schemes of operation scenarios, kinematic interactions, forward and inverse kinematic, constraints, dynamic parameters, consolidation of the dynamic equation, real experimentation and positioning simulation.

### 2.1 Preliminary analysis

The robot MMR12-EOD is considered by being able to move on a surface by the action of its wheels mounted in the robot and touching the surface. The wheels are mounted on devices that allow relative movement between its attached point (point of guidance) and a

surface (the floor), at which it must have a unique rolling contact [6-7]. It is assumed that the robot is being built with rigid mechanisms, that there is an link guided by every wheel, that all the axes guided are perpendicular to the floor, that the surface of the motion is a plane, and that there is no sliding with the rolling surface and that the friction is sufficiently small to allow the rotation of any wheel about the guided axis [8-10]. Sliding with the surface is the biggest problem during the moment of establishing a location with high accuracy. Figure 1 shows that the mobile platform has 4-DOF, that the manipulator has 4-DOF and that the added subsystem does too.

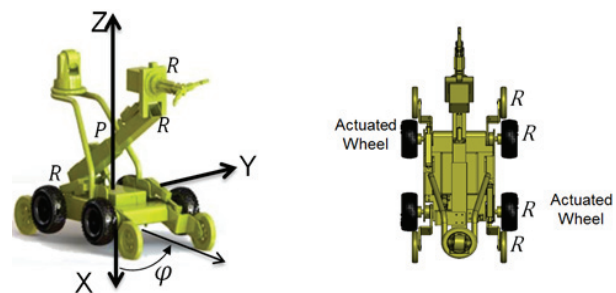


Figure 1. Robot MMR12-EOD

The average velocity of the robot MMR12-EOD is 0.5 m/s and it is required to support a load of 10 kg at its end effector. These features, as well as the critical parameters and the kind of system (non-holonomic) are used as a base in order to form the master map.

### 2.2 Master map

The master map is a diagram that shows the development of the mathematical model, in which is represented the subsystems and homogenous transformations of the mobile manipulator. Described first are both the external and internal constraints, being those external constraints which are related to the operating environment. As such, the terrain is considered as the localization of its local coordinates with respect to global coordinates. The internal constraints are determined according to the non-holonomy of the mobile platform. Afterwards, the scheme with the nomenclature M-MMR (adding the other subsystem) is classified, where M is the manipulator and MMR is the mobile to which is added the other subsystem, like the lifting arms or any subsystem. In the case where the additional subsystem is a manipulator (operating cooperatively and located in the same origin as that of the principal manipulator), then the homogenous transformations of this subsystem will relate to the origin coordinate "0" rather than being related to the local coordinate "C". The master map has the stages related to the subsystems for the mobile manipulator MMR12-EOD in relation to the tasks of orientation, approaching and manipulation; in this case, the mobile manipulator has an added subsystem formed by two coupled lifting arms (B. A.) at which are considered the lifting and climbing tasks

[11-14]. In order to model the robot MMR12-EOD, seven stages in five real operation scenarios are considered [7], at which the assessed behaviour of the full system with and without load is considered. For the robot in the present work, the stages are:

- The additional subsystem is considered in the neutral position and in operation with respect to the local coordinate "C". This subsystem is called "A". This stage is omitted if the manipulator has no additional subsystem.
- The manipulator uses just its degrees of freedom to perform tracking trajectories tests in relation to the coordinate "0", which is the base of the manipulator.
- The mobile platform is moved forward with the manipulator mounted and performing a tracking trajectory test from the coordinate "C" to the global coordinate "G4".
- Considering the coupled system without allowing the advance of the mobile platform, the manipulator realizes the test of the tracking trajectory, assuming that the mobile platform rotates about its axis with respect to the local coordinate "C".
- The mobile platform is moved forward with the manipulator coupled while performing a tracking trajectory test from the coordinate "C" with respect to the global coordinate "G4".
- The coupled system is moved in a straight line, moving its manipulator in relation to the end effector with respect to "G4".
- The coupled system is subjected to the tests for tracking the trajectory in relation to the end effector with respect to the coordinate "G4".

### 2.3 Diagram of the position and orientation

The general description for the orientation and position of the system is described by the fourth transformation of the global coordinates with respect to GG, as shown in figure 2.

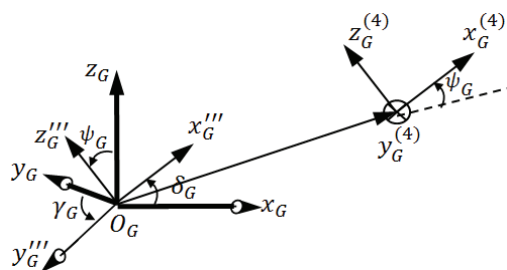


**Figure 2.** Fourth Transformation of the global coordinates with respect to the global coordinates

### 2.4 Homogeneous transformation graph (HTG)

The third step of the proposed methodology is the homogenous transformation graph that, in a modular way, allows the organization of the subsystems that

constitute the mobile manipulator plus the added subsystem. This graph is an extension of the graph for obtaining the kinematics of the manipulators proposed by Robert Pauli, in 1983 [15], and used in several works by Tadeusz Skodny [16, 30] in order to perform the same applications. The extension of Pauli's graph allows us to get the homogenous transformation graph and the kinematic modelling of wheeled mobile manipulators with any additional subsystem. These transformations are the central part of the methodology because they provide the relations with the coordinates "0" of manipulator and "C" of the mobile platform, as well as the transformations of the wheels and the lifting arms in relation to "C" and "C" with respect to "G4", as shown in figure 3. Afterwards, coordinates systems to the selected points that allow us to obtain the coupled kinematic modelling of full system are assigned.

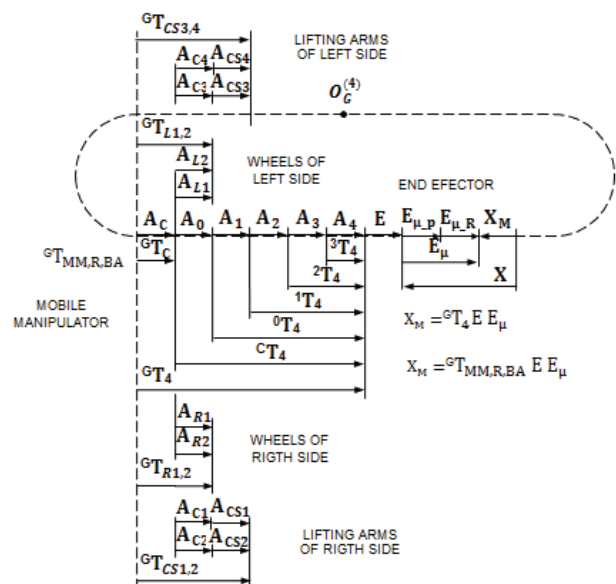


**Figure 3.** HTG for mobile manipulators

### 2.5 Schemes for the kinematics of the operation scenarios

In order to realize the schemes for the kinematics of five real operational scenarios of the MMR12-EOD robot, it is necessary to consider its design parameters.

### 2.6 Interaction kinematics

Table 2 presents the parameters of the interaction kinematics obtained from the coupling of the subsystems of the robot MMR12-EOD.

### 2.7 Forward and inverse kinematics

#### 2.7.1 Forward kinematics

Based on the homogenous transformation graph and the table of the kinematic interactions, we develop the forward kinematics, starting with the coordinate "C", and from here describe the transformations of the wheels, the

lift arms and the manipulator, considering the end effector "E" with the load "E $\mu$ ", as shown in figures 4 and 6 [17, 28-30].

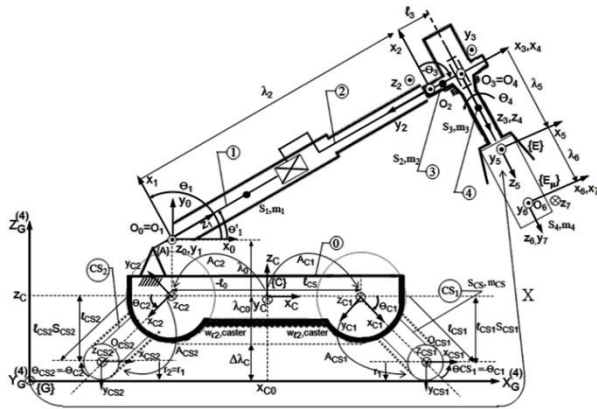


Figure 4. Lateral view of the MMR12-EOD in the lifting position

#### a) Mobile platform

The homogenous transformation of the mobile platform is given by  $A_C = (x_G^{(4)} y_G^{(4)} z_G^{(4)} \rightarrow x_C y_C z_C)$ , where the parameters are:  $A_C: x_{C0} = \text{var}, y_{C0} = \text{var}, z_C = \text{var} = \lambda_{C0} + \Delta\lambda_C, z_{C0} = \lambda_{C0} = \text{const} > 0, \theta_{C1} = \text{var}, l_{CS1} = \text{const} > 0, \varphi = \text{var}$ . The increment of  $\lambda_C$  depends upon the following relationship:

$$\Delta\lambda_C = \begin{cases} l_{CS1}S_{C1} - \lambda_{C0} + r \\ \text{for } l_{CS1}S_{C1} - \lambda_{C0} + r \geq 0, r = \text{constant} > 0 \\ 0 \text{ for another case} \end{cases} \quad (1)$$

Then the transformation of the local coordinate,  $GT_C = A_C$  and the transformations for the wheels of the right side and the left side,  $GT_R = A_C A_R$  and  $GT_L = A_C A_L$  are obtained [29-30].

#### b) Lifting arms

The transformations of the lifting arms are developed with respect to the local coordinate "C". The parameters for the lifting arm of the right front side are given by:  $A_{CS1}: \theta_{CS1} = \text{var}, l_{CS1} = \text{const} > 0$ . Therefore, the transformation of first arm in relation to the global coordinates is expressed as  $GT_{CS1} = A_C A_{C1} A_{CS1}$ . In a similar way, the relations for the second, third and fourth lifting arms are obtained.

#### c) Manipulator

The homogenous transformations of its 4-DOFs with respect to the coordinate "0" in relation to the coordinate "C" are now presented. The homogeneous transformation from "C" to "0",  $A_0 = (x_C y_C z_C \rightarrow x_0 y_0 z_0)$ , depends upon the following parameters:  $\theta_0 = 0^\circ, \lambda_0 = \text{const} > 0, l_0 = \text{const} < 0, \alpha_0 = 90^\circ$ . The transformation  $A_1 = (x_0 y_0 z_0 \rightarrow x_1 y_1 z_1)$ , depends upon the following parameters:  $\theta_1 = \text{var}, \lambda_1 = 0, l_1 = 0, \alpha_1 = 90^\circ$ . The transformation  $A_2 = (x_1 y_1 z_1 \rightarrow x_2 y_2 z_2)$ , depends upon the

following parameters:  $\theta_2 = 0^\circ, \lambda_2 = \text{var}, l_2 = 0, \alpha_2 = -90^\circ$ . The transformation  $A_3 = (x_2 y_2 z_2 \rightarrow x_3 y_3 z_3)$  depends upon the following parameters:  $\theta_3 = \text{var}, \lambda_3 = 0, l_3 = \text{const} > 0, \alpha_3 = 90^\circ$  and the transformation  $A_4 = (x_3 y_3 z_3 \rightarrow x_4 y_4 z_4)$  depends upon the following parameters:  $\theta_4 = \text{var}, \lambda_4 = 0, l_4 = 0, \alpha_4 = 0^\circ$ .

The transformations of the end effector in relation to the fourth degree of freedom of the manipulator are given by  $E = (x_4 y_4 z_4 \rightarrow x_5 y_5 z_5)$ , where  $E = \text{Trans}(0, 0, \lambda_5)$  and its parameters are  $E: \theta_5 = 0^\circ, \lambda_5 = \text{const} > 0, l_5 = 0, \alpha_5 = 0^\circ$ . In order to obtain transformations that connect the load with the end effector, these are obtained by the relationship  $E_\mu = E_{\mu_P} E_{\mu_R}$ , where  $E_\mu$  is the total load, constituted by  $E_{\mu_P}$  and  $E_{\mu_R}$ , which are the prismatic load and the rotational load, respectively [18]. The parameters of the prismatic joint are as follows:  $E_{\mu_P}: \theta_6 = 0^\circ, \lambda_6 = \text{const} > 0, l_6 = 0, \alpha_6 = 0^\circ$ . The parameter of the rotational joint are as follows:  $E_{\mu_R}: \theta_7 = 0^\circ, \lambda_7 = 0, l_7 = 0, \alpha_7 = 90^\circ$ .

Then, the transformations from the joints of the manipulator are multiplied so that the transformation of the manipulator is  $T_4$ , using the trigonometric simplification  $\cos(A + B) = C_A C_B - S_A S_B = C_{AB}$ ,  $\sin(A + B) = C_A S_B + S_A C_B = S_{AB}$  obtained by the transformation from the manipulator to the global coordinates given by  $GT_4 = A_C T_4$ . The transformation of the end effector with the load is determined by  $E_\mu = E_{\mu_P} E_{\mu_R}$ . Finally, we obtain the homogeneous transformation from the load "X" in the end effector in relation to the global coordinates described by equation 2 [19].

$$X_M = GT_4 E E_\mu =$$

$$\begin{bmatrix} A & D & G & x_C + C_C(S_1\lambda_2 + l_3C_{13} - l_0) + C_C\lambda_5S_{13} + C_C\lambda_6S_{13} \\ B & E & H & y_C + S_C(S_1\lambda_2 + l_3C_{13} - l_0) + S_C\lambda_5S_{13} + S_C\lambda_6S_{13} \\ C & F & I & z_{C0} + \Delta\lambda_C + \lambda_0 - \lambda_5C_{13} - C_1\lambda_2 + l_3S_{13} - \lambda_6C_{13} \\ 0 & 0 & 0 & 1 \end{bmatrix} \quad (2)$$

where:

$$A = S_4S_C + C_C C_{13} C_4, B = S_C C_{13} C_4 - C_C S_4, C = S_{13} C_4, D = C_C S_{13}, E = S_C S_{13}, F = -C_{13}, G = C_C C_{13} S_4 - C_4 S_C, H = S_C C_{13} S_4 + C_4 C_C, I = S_{13} S_4.$$

#### 2. 7. 2 Inverse kinematics

Here, the equations that connect the Cartesian coordinates of the task space in relation to the joint parameters are described in order to carry the end effector from the mobile manipulator to the mentioned Cartesian coordinates. The inverse kinematics were developed using the homogeneous transformations of the equations 3 to 11 from the scheme for forward and the inverse kinematics, which is represented by figure 5.



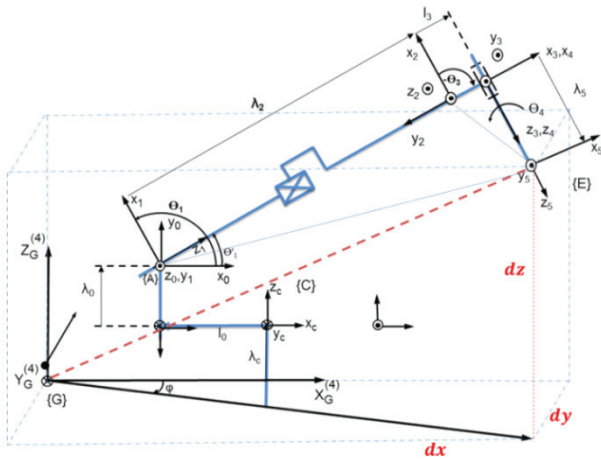


Figure 5. Scheme for the inverse kinematics

$$\varphi = \tan^{-1} \left( \frac{dy}{dx} \right) \quad (3)$$

$$\theta_3 = \cos^{-1} \left[ \frac{dx^2 + dy^2 + dz^2 - \lambda_2^2 - \lambda_5^2}{-2 \lambda_2 \lambda_5} \right] \quad (4)$$

$$\lambda_2 = \frac{dz + \lambda_0 - \lambda_5 C_3 + l_3 S_3}{C_3} \quad (5)$$

$$E = \tan^{-1} \left( \frac{l_3}{\lambda_5} \right); K = 180 - 90 - E1; h = \left( \frac{l_3}{S_E} \right); \quad (6)$$

$$P = 180 - K - q_3; r = \sqrt{h^2 + d_2^2 - [2hd_2C_{P1}]}; \quad (7)$$

$$d = \cos^{-1} \left( \frac{(h^2 + r^2 - d_2^2)}{2hr} \right); q'_1 = 180 - P - d1; \quad (8)$$

$$q''_1 = \sin^{-1} \left( \frac{d_z + d_o - d_c}{r} \right); q_1 = q'_1 + q''_1 \quad (9)$$

$$x_c = d_x - C_c(\lambda_2 S_1 - l_0 + l_3 C_{13} + \lambda_5 S_{13}) \quad (10)$$

$$y_c = d_y - S_c(\lambda_2 S_1 - l_0 + l_3 C_{13} + \lambda_5 S_{13}) \quad (11)$$

## 2. 8 Constraints

The differential kinematics in relation to  $Z_G^{(4)}$  is developed based on the non-holonomy constraint - namely, it does not have an integrable solution and it represents more DOFs than the controllable DOFs [20-21] in relation to figure 6. In order to obtain the relations of the velocities from the system, we considered that the orientation angles in relation to the global coordinates are,  $(x_G, \delta_G)$ ,  $(y_G, \varphi_G)$  and  $(z_G, \gamma_G)$ , assuming that the position and orientation of the local reference in relation to the global reference is constant in the movement of the robot and  $\dot{\theta}_{C1} = 0, \dot{\theta}_{CS1} = 0$ . Table 1 shows the constraints of the equations [22-25].

$$q = [x_{c0} \ y_{c0} \ \varphi_c \ \theta_r \ \theta_l \ z_{c0} \ \theta_{C1} \ \theta_{CS1} \ \theta_1 \ d_2 \ \theta_3 \ \theta_4]^T \quad (15)$$

$$J = \begin{bmatrix} -\sin\varphi & \cos\varphi & 0 & 0 & 0 & 0 & 0 & 0 & 0 & 0 & 0 & 0 \\ -\cos\varphi & -\sin\varphi & -b & r & 0 & 0 & 0 & 0 & 0 & 0 & 0 & 0 \\ 0 & 0 & -1 & \frac{r}{2b} & -\frac{r}{2b} & 0 & 0 & 0 & 0 & 0 & 0 & 0 \end{bmatrix} \quad (16)$$

It is known that  $J(q)\dot{q} = 0$  and that  $J(q)$  is a square matrix, then:  $J_1^{-1} = \frac{1}{|J_1|} [\text{adj}(J_1)]^T, [\text{adj}(J_1)]^T$  because the

determinant of  $J_1$  is  $|J_1| = -1$ , and so the mobile manipulator has good manipulability according to the mobile platform [27] -  $J(q) = [J_1(q), J_2(q)]$ . Finally,  $J_{12}(q) = -J_1^{-1}(q)J_2(q)$ .

The mobile platform must move in the direction of its axis of symmetry with respect to the ground, where $(x_{c0}, y_{c0}, z_{c0})$ are the coordinates of its centre of mass and $\varphi$ is the heading angle of the platform measured from $X_G^{(4)}$ [26].	$\dot{y}_{c0} \cos\varphi - \dot{x}_{c0} \sin\varphi = 0 \quad (12)$
The other two constraints are the rolling constraints - i. e., the driving wheels do not slip - where $\theta_r, \theta_l$ are the angular displacements of the right and left wheels, respectively [26].	$\dot{x}_{c0} \cos\varphi + \dot{y}_{c0} \sin\varphi + \dot{\varphi} b = \dot{\theta}_r r \quad (13)$ $\dot{\varphi} = \frac{r}{2b} (\dot{\theta}_r - \dot{\theta}_l) \quad (14)$

Table 1. Constraint equations to the robot MMR12-EOD

## 2. 9 Dynamic parameters

The dynamic model was done using Lagrange's computational algorithm, based on the homogeneous transformations and the interactions table [28]. We will use the letter L to depict the steps. L1 is described every link in the interactions table. On L2 is established the homogeneous transformations in the G. T. H. and the forward kinematics. On L3 is developed the matrix  $U_{ij}$ , L4 the matrix  $U_{ijk}$ . On L5 is obtained the pseudo-inertia matrix for each link and on L6 is obtained the matrix of inertia  $M(q) = [d_{ij}]$ . On L7 is developed the terms  $h_{ikm}$ , and in L8 is obtained the matrix of the Coriolis and the centrifuge  $V(q, \dot{q}) = [h_i]^T$ . On L9 is obtained the matrix of gravity  $G(q) = [c_i]^T$ . As, we obtain the dynamic equation 17 on L10.

$$M(q)\ddot{q} + V(q, \dot{q})\dot{q} + G(q) = E(q)\tau - A^T(q)\lambda \quad (17)$$

## 2. 10 Consolidation of the dynamic equation.

The two columns from  $S(q)$  are the null space from  $A(q)$  and are linearly independent. It presents  $\dot{q}$  as linear combination of two columns from  $S(q)$ ,  $\dot{q} = S(q)v$ . Deriving  $\dot{q}$  we have  $\ddot{q} = S(q)\dot{v}(t) + \dot{S}(q)v(t)$  and replacing it in equation 14 gives as the result of equations 21 and 22:

$$M(q) = \begin{bmatrix} d_{11} & \dots & d_{112} \\ \vdots & \dots & \vdots \\ d_{121} & \dots & d_{1212} \end{bmatrix} \ddot{q} + \begin{bmatrix} h_1 \\ \vdots \\ h_{12} \end{bmatrix} \dot{q} + \begin{bmatrix} c_1 \\ \vdots \\ c_{12} \end{bmatrix} = \begin{bmatrix} 0 & 0 \\ \vdots & \vdots \\ 1 & 0 \\ 0 & 1 \\ \vdots & \vdots \\ 0 & 0 \end{bmatrix} \begin{bmatrix} \tau_x \\ \tau_4 \end{bmatrix} - \begin{bmatrix} -S_c & C_c & 0 & 0 & 0 & \dots & 0 \\ -C_c & -S_c & -b & r & 0 & \dots & 0 \\ 0 & 0 & b & 0 & r & \dots & 0 \end{bmatrix} \quad (18)$$

$$\ddot{q} = M(q)^{-1} [E(q)\tau - A^T(q)\lambda - V(q, \dot{q})\dot{q} - G(q)] \quad (19)$$

$$S(q) = \begin{bmatrix} -S_c & C_c & 0 & 0 & 0 & \dots & 0 \\ -C_c & -S_c & -b & r & 0 & \dots & 0 \\ 0 & 0 & b & 0 & r & \dots & 0 \end{bmatrix} \quad (20)$$

$$S^T(q) \left( M(q)S(q)\dot{v}(t) + M(q)\dot{S}(q)v(t) + V(q, \dot{q})\dot{q} + G(q) \right) = (E(q)\tau - A^T(q)\lambda)S^T(q) \quad (21)$$

$$S^T(q)(M(q)S(q)\dot{v}(t) + M(q)\dot{S}(q)v(t) + V(q, \dot{q})\dot{q} + G(q)) = \tau \quad (22)$$

Is verified that  $M(q)$  complies with  $n=m$  (square),  $M^T(q)=M(q)$  (symmetric). It is not singular ( $\det(M(q)) = 8.0644e + 021 > 0 = \det(M(q)^T) = 8.0644e + 021 > 0$ ;  $d_{11} = 0.219 > 0$ ), and therefore is inverse.  $M^{-1}(q) \exists$ ;  $M^{-1}(q) = (M^{-1}(q))^{-1} > 0$ . It is also positive definite, in that  $M_{11}(q) > 0$  for all  $q$  and its determinant( $M(q)$ )  $> 0$ .

### 3. Real experiment and positioning simulation

The real experiment and the simulation of positioning from the mobile manipulator is done according to the 5 real operation tasks. In order to realize these activities, the control strategy published by Yamamoto was used [29] in the paper dedicated to the control and coordination of movement from mobile manipulators in 2004. Using the vector in the state space  $x = \begin{bmatrix} q^T & v^T \end{bmatrix}^T$ , we can represent the constraints and the motion's equations from the mobile manipulator in the state space:

$$\dot{x} = \begin{bmatrix} Sv \\ f_2 \end{bmatrix} + \begin{bmatrix} 0 \\ (S^T MS)^{-1} \end{bmatrix} \tau \quad (23)$$

where  $f_2 = (S^T MS)^{-1}(-S^T MSv - S^T V)$ . This equation is simplified in order to apply the following linear feedback:  $\tau = S^T MS(u - f_2)$ . Then, it could assume a new input  $u$ , which will linearize equation 23. Considering the linearization, it could be used in the desired trajectory  $y^d$  in order to feedback the error  $e = y^d - y$ :

$$\ddot{y} = v = \ddot{y}^d + K_d(\dot{y}^d - \dot{y}) + K_p(y^d - y) \quad (24)$$

From equation 24,  $v$  is obtained and then  $u$  and, therefore,  $\dot{x}$ . Finally, by integration,  $x$  can be obtained.

a) Orientation (stage 2, task 1). The driving wheels are located on the left side at the front and right side rear, the alternate movement  $v_r = -v_r$  allows the rotation about axis  $z$  in the reference ratio of  $\varnothing$  1130 mm. This is using the transformation  $GT_C = A_C$  and  $q_M = [\varphi_C \ \theta_r \ \theta_l]^T$ . Therefore, it is assumed that the movement is in the horizontal plane [13], that the contact wheel is at one point, that the wheels are not deformable, that there is pure rotation at the contact point  $v = 0$ , that there is no slippage, and that the axis direction is orthogonal to the surface. The wheels are connected by a rigid body (chassis).

b) Approximation / trajectories tracking (stage 4, task 2). The system executes the tracking of the desired trajectory,

based in the transformation  $GT_C = A_C$ . The mobile platform is moved according to this equation,  $q_{MR} = [xyz\varphi_C \ \theta_r \ \theta_l]^T$ .

c) Manipulation (stage 4, task 3). In the rank  $x=2.5$ ,  $y=2.5$  and  $z=1.5$  m, the kinematics is given by  $X_M = GT_4 E_\mu$  by the equation  $q_M = [\varphi_C \ \theta_1 d_2 \theta_3 \theta_4]^T$ .

d) The lifting of the mobile manipulator in the rank from 0.15 up to 0.52 m based on the transformation  $GT_C = A_C$ ,  $z$  is given by  $z_C = \text{var} = \lambda_{C0} + \Delta\lambda_C$ ,  $z_{C0} = \lambda_{C0} = \text{constant} > 0$ ,  $\theta_{C1} = \text{variable}$ ,  $l_{CS1} = \text{constant} > 0$ ,  $\varphi = \text{variable}$ , where the increment  $\Delta\lambda_C$  of  $z$ , depends upon the lifting arms.

e) The lifting arms climb in the rank from 0.15 up to 0.47 m. The mobile manipulator with a mass  $m$  is moved on the sloped surface at an angle  $\psi$ , with respect to the horizontal, given by the transformation  $CT_{CS1}$ , and the equation  $F_{\text{ascenso}} = mg(\sin\psi + \mu\cos\psi)$ , where  $g$  is gravity when  $\theta_{CS} > 60^\circ$ ,  $\lambda_C + (\Delta_C = l_{CS1} + \sin\theta_{CS})$ , in order to realize the climbing task.  $\lambda_C$  is variable and depends upon  $\theta_{CS}$ .

### 4. Results

From the forward kinematics, the reference values for every task were taken. The parameters of the coordinate local "C" which is the base for obtaining the reference values are as follows:  $A_C: x_{C0} = 2, y_{C0} = 2, z_C = \lambda_{C0} + \Delta\lambda_C, z_{C0} = \lambda_{C0} = 0.15, \theta_{C1} = \frac{\pi}{2}, l_{CS1} = 0.44, \varphi = \frac{\pi}{4}, \varphi = 20\pi$ .

$$\Delta\lambda_C = \text{variable} = \begin{cases} l_{CS1}S_{C1} - \lambda_{C0} + r \\ \text{for } l_{CS1}S_{C1} - \lambda_{C0} + r \geq 0, r = 0.08 \\ 0 \text{ for another case} \end{cases} \quad (25)$$

a) Equation 26 is the transformation of the mobile platform rotating about its own axis:

$$GT_C = \begin{bmatrix} 1 & 2.4493e-015 & 0 & 0 \\ -2.4493e-015 & 1 & 0 & 0 \\ 0 & 0 & 1 & 0.15 \\ 0 & 0 & 0 & 1 \end{bmatrix} \quad (26)$$

b) Equation 27 is the transformation of the platform according to these parameters:  $x_C = 2, y_C = 2, \lambda_{C0} = 0.15, \varphi_C = \frac{\pi}{4}, \theta_R = 2\pi, \theta_L = -2\pi, b = 0.4, \Delta\lambda_C = 0$ .

$$GT_C = A_C = \begin{bmatrix} 0.7071 & -0.7071 & 0 & 2 \\ 0.7071 & 0.7071 & 0 & 2 \\ 0 & 0 & 1 & 0.15 \\ 0 & 0 & 0 & 1 \end{bmatrix} \quad (27)$$

c) Equation 28 is the transformation of the manipulator with the end effector:  $x_C = 2, y_C = 2, \lambda_{C0} = 0.15, \varphi_C = \frac{\pi}{4}, \lambda_0 = 0.16, l_0 = 0.33, \theta_1 = \frac{3\pi}{4}, \lambda_2 = 1.4, \theta_3 = -\frac{\pi}{2}, l_3 = 0.15, \theta_4 = \frac{\pi}{2}, \theta_{C1} = \frac{\pi}{2}, l_{CS1} = 0.44, r = 0.08, \lambda_5 = 0.38, \lambda_6 = 0.25$ :

$$X_M = GT_4 E E_\mu = \begin{bmatrix} 0.7071 & 0.5000 & 0.5000 & 2.8567 \\ -0.7071 & 0.5000 & 0.5000 & 2.8567 \\ 0 & -0.7071 & 0.7071 & 1.3305 \\ 0 & 0 & 0 & 1 \end{bmatrix} \quad (28)$$

d) Equation 29 is the transformation at the time that the platform is lifting:  $x_C = 0, y_C = 0, \theta_{C1} = \frac{\pi}{2}$ :

$$GT_C = A_C = \begin{bmatrix} 0.7071 & -0.7071 & 0 & 0 \\ 0.7071 & 0.7071 & 0 & 0 \\ 0 & 0 & 1 & 0.5200 \\ 0 & 0 & 0 & 1 \end{bmatrix} \quad (29)$$

e) Equation 30 is the transformation corresponding to climbing:  $x_C = 0, y_C = 0, \lambda_{C0} = 0.15, \varphi_C = \frac{\pi}{4}, \theta_{C1} = \frac{\pi}{2}, \theta_{CS1} = -\frac{\pi}{2}, d = 0.35, l_{CS} = 0.33, l_{CS1} = 0.44, r = 0.10$ .

$$GT_{CS1} = \begin{bmatrix} 0.7071 & 0 & -0.7071 & 0 \\ 0.7071 & 0 & 0.7071 & 0 \\ 0 & -1 & 0 & 0.47 \\ 0 & 0 & 0 & 1 \end{bmatrix} \quad (30)$$

Taking the reference values, several simulations using equation 30 for the real operational scenarios were carried out, where the errors and performance index were obtained, as shown in tables 2 and 3.

Tracking trajectory about its geometric centre.	Sampling time: $t_m = 200$ s. The reference C is located on these coordinates: $y_{desired} = 0$ $x_{desired} = 0$ Mean error of 40 mm.
Tracking trajectory of the sinusoidal curve.	$t_m = 200$ s. The reference is located on these curves: $y_{desired} = 30 \sin(0.25 t)$ $x_{desired} = 40 \cos(0.25 t) + 2.5 t$ Mean error of 2.37 mm.

Table 2. Tasks for orientation and the tracking trajectory

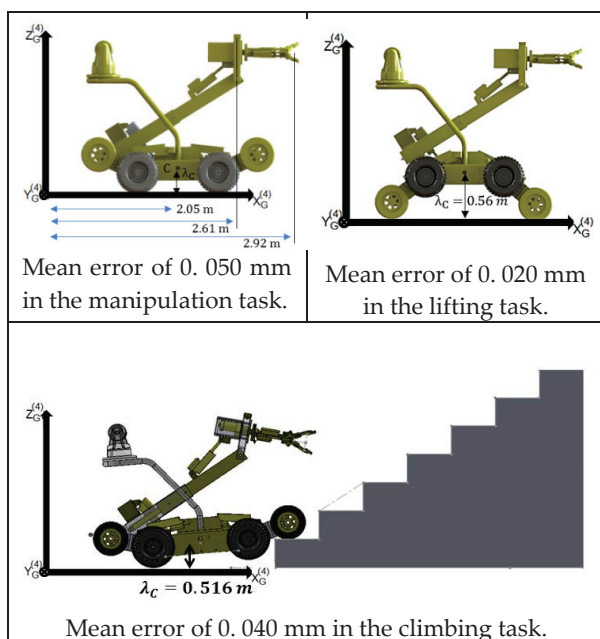


Table 3. Tasks for manipulation, lifting and climbing

In table 4, the results of real experiments in the mobile manipulator are shown, focusing on the maximum and minimum errors according to the reference values.

30 samples	Deviations	
1. In the test for orientation the next errors were taken:	Error min. 40 mm	Error max. 80 mm.
2. Approaching (trajectories tracking).	Error min. 0.5 mm	Error max. 8 mm.
1. Manipulation (positioning).	Error min. 0.5 mm	Error max. 8 mm.
2. Lifting.	Error min. 4 mm	Error max. 6 mm.
3. Climbing.	Error min. 4.6 mm	Error max. 8 mm.

Table 4. Real experiments for the manipulation, lifting and climbing tasks.

In figure 6, we see the mobile manipulator in a real experiment approaching and positioning the end effector in the target.

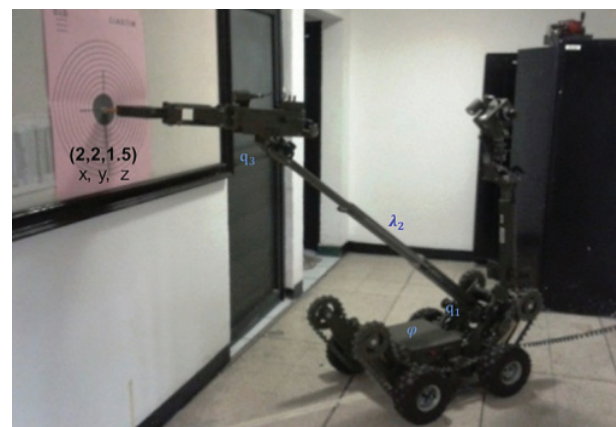


Figure 6. Mobile manipulator in a real experiment

## 5. Discussion

The real experiment was carried out on the floor inside a laboratory, which helped in the measurement of the registered parameters; however, measurements in rough ground were not taken due to a lack of adequate methods and instrumentation for the corresponding measurements of its parameters. The comparison of the errors of the simulations and the real experiments of the 5 evaluated tasks are presented in table 5. As many as 30 samples were taken for each task, which validates the kinematic modelling.

In table 6 is shown the differences in errors between the simulation and the real experiments of the 5 evaluated tasks. The figures are described in the Gaussian bell form, with the results of the simulation in blue and the experiment in red, including the mean and the R. M. S error.

Task	Performance [mm]			
	Simulation ( $\bar{e}$ y RMS)		Real system ( $\bar{e}$ y RMS)	
Orientation.	40 and 40. 161		60 and 60. 0922	
	Error due to the wheel slipping on the floor.			
Approaching.	2. 37 and 2. 376		6. 5 and 6. 5236	
	The 2 tests were performed at 0. 5 m /s.			
Manipulation.	0. 050 and 0. 051		4. 25 mm and 4. 25002	
	This is due to slip of wheels on the floor.			
Lifting.	0. 020 and 0. 02144		5 and 5. 037658	
	Due to adjustment and weight of system.			
Climbing.	0. 040 and 0. 040743		6. 3 and 6. 30918	
	This is due to the deformation of the rear wheels and its adjustment, in addition to its weight.			
	8. 497	8. 5299	16. 41	16. 447
	With load		Without load	
Dynamic analysis with software CAE	The mass centre varies in $\varnothing$ 60.		The mass centre varies in $\varnothing$ 40.	
	The greatest variation occurs in Z.			
	The stress due to a load of 14 kpa.		The stress due to a load of 7 kpa.	
	The deformation of $\lambda_2$ is 1. 055.		The deformation of $\lambda_2$ is 0. 03.	
	It was validated to the fullest extension and in the normal state of the prismatic joint.			
According to the manual of explosives, deactivation [24] must be considered with a maximum handling error of 10 mm.				

**Table 5.** Simulation and real experiments for the tasks.

Comparison of the simulation and the real experiment			
Tasks		Difference	
1. Orientation.	$\bar{e}$	20 mm	
	RMS	19.94 mm	
2. Approaching.	$\bar{e}$	4.12 mm	
	RMS	4.147 mm	
3. Handling.	$\bar{e}$	4.2 mm	
	RMS	4.19 mm	
4. Lifting.	$\bar{e}$	4.98 mm	
	RMS	5.01 mm	
5. Climbing.	$\bar{e}$	6.26 mm	
	RMS	6.28 mm	

**Table 6.** Errors between the simulation and the real experiment.

The orientation error is very large due to wheel slippage on the ground, as well as the tracking of the trajectory where the trajectory is a point referenced by the mass centre of the mobile manipulator; the aforementioned variations are due to the compensation of the control of the non-holonomy of the system caused by the non-integrable solutions of the wheels.

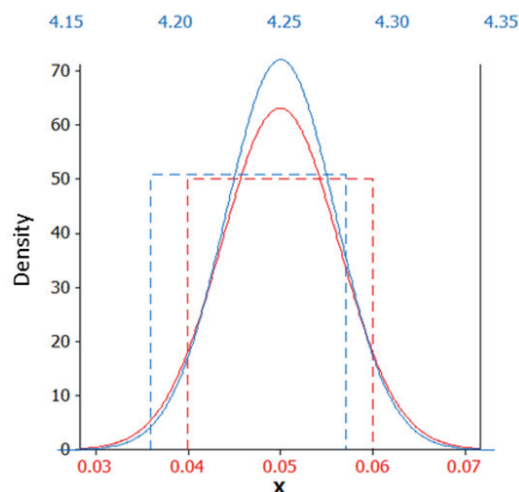


**Figure 7.** Error simulation against the error of the real experiment for the manipulation task

## 6. Conclusion

A methodology for the positioning of the multi-articulated mobile manipulator by means of the development of a kinematical model is defined, explained and assessed, where the use of a novel scheme to devise the homogeneous transformations achieves the given structure for the forward kinematics. The methodology has the following advantages: (1) it provides a big picture for mechatronic design when it develops the modelling and simulation of the mobile manipulator; (2) it simplifies the estimation of the homogenous transformation when it is required; (3) it allows the determination of the parameters of interaction when it is necessary to make the schemes in a coupled way; (4) it is easy for kinematic modelling when any added subsystem is incorporated in the analysis of the performance index based on the error of the real operational scenarios:

The simulations have an average error RMS of 3.47 mm with regard to the references values, while the real experimentations have an error RMS of 7.91 mm. These are permissible errors in relation to the error of 10 mm, which is specified in the tasks for the deactivation of explosives [30]. The maximum deformation of the manipulator with a load of 10 kg was 1 mm.

The major advantages of this proposal in comparison with previous work are considered, such as the contributions of this paper: the development of kinematic modelling in a coupled way for a wheeled mobile



manipulator with 12-DOF, the extension of homogeneous transformation graphs which organize in a modular way the transformations of every link so as to obtain the kinematics of the mobile manipulators and the proposed methodology for modelling the positioning in real operational scenarios.

As to future work, by means of a visual feedback system, will be determined the position of the explosive device incorporating a vision system to detect the coordinates of targets, placing some sensors at the end effector for use in different kinds of manipulation based in the device's form, and finally implementing the proposed modelling methodology in the design of mobile systems with different manipulators.

## 7. Acknowledgements

The authors would like to acknowledge the Centro de Ingeniería y Desarrollo Industrial (CIDESI) [30] for funding this work.

## 8. References

- [1] Zúñiga L. Diseño de un Effector Final para Manipulación de Artefactos Explosivos. Engineering Thesis, Engineers Military School from Mexican Army, 2003.
- [2] Krus P. Distributed Techniques for Modelling and Simulation of Engineering Systems. Technical Report, Department of Mechanical Engineering Linköping University, Linköping, Sweden, 2000.
- [3] Korayem M. H., Baniroostam T. Design, Modeling and Experimental Analysis of Wheeled Mobile Robots. 3rd IFAC Symposium on Mechatronic Systems, 2/a. ed. Vol. 12, September 2004: 821-228.
- [4] Li Li, Fei-Yue W. Advanced Motion Control and Sensing for Intelligent Vehicles. Springer, University of Arizona, U. S. A., 2007; ISBN: 0-387-44407-6.
- [5] Birta G., Louis A. G. Modelling and Simulation Exploring Dynamic System Behaviour. Springer-Verlag, London, U. K., 2007; ISBN-10: 1-84628-621-2.
- [6] Josephs H., Huston R. Dynamics of Mechanical Systems. CRC Press LLC. U. S. A., 2004.
- [7] Bayle B., Fourquet J. Y., Renaud M. Nonholonomic Mobile Manipulators: Kinematics, Velocities and Redundancies. Journal of Intelligent and Robotic Systems, Vol. 36, January 2003.
- [8] Yamamoto Y., Yun X. Coordinating Locomotion and Manipulation of a Mobile Manipulator. IEEE Transactions on Automatic Control, 6th. Ed., Vol. 39, June 1994.
- [9] Paul R. P. Robot Manipulators: mathematics, programming and control. MIT Press, Massachusetts, 1981; ISBN: 0-262-16082.
- [10] Skodny T. Forward and Inverse kinematics of IRb-6 Manipulator. Mach. Theory, Pergamon Press, London, 1995; 30(7): 1039-1056.
- [11] Pavlov V., Timofeyev A. Construction and stabilization of programmed movements of a mobile robot-manipulator. Engineering Cybernetics, 1976; 14(6):70-79.
- [12] Dubowsky S., Tanner A. B. A study of the dynamics and control of mobile manipulators subjected to vehicle disturbances. In Robotics research: 4th International Symposium, 1988: 111-117.
- [13] Arai T. Robots with integrated locomotion and manipulation and their future. IROS, Osaka, Japan, November 1996: 541-545.
- [14] Ghaffari A., Meghdari A., Naderi D., Eslami S. Stability enhancement of mobile manipulators via soft computing. International Journal of Advanced Robotic Systems. 2004; 3(3): 191-198.
- [15] Aviles J. A. Z., Pedraza J. C., Gorrostieta E., García-V L. H. Development of a Mechatronic Unit applied to the Manipulation of Explosives. International Conference on Electrical Engineering, Computing Science and Automatic Control, CCE, 2008; ISBN: 978-1-4244-2499-3.
- [16] Zúñiga L. A., Pedraza J. C., Gorrostieta E., Ramos J. M. Analysis of Dynamic Behavior of an EOD Mechatronic Unit. International Conference on Electronics, Robotics and Automotive Mechanics Conference, CERMA, 2009.
- [17] Choset H., Lynch K. M., Hutchinson S., Kantor G., Burgard W., Kavraki L. E., Thrun S. Principles of Robot Motion: Theory, Algorithms, and Implementation. MIT Press, USA, 2005; ISBN: 1098765432.
- [18] Bayle B., Fourquet J. Y., Renaud M. Manipulability of Wheeled Mobile Manipulators: Application to Motion Generation. International Journal of Robotics Research, 2003; 22(708): 565- 581.
- [19] Velinsky S. A., Gardner J. F. Kinematics of mobile manipulators and implications for design. Journal of Robotics Systems, 2000: 309-320.
- [20] Tang C. P., Bhatt R. M., Abou-Samah M., Krovi V. A Screw-Theoretic Analysis Framework for Payload Transport by Mobile Manipulator Collectives. IEEE/ASME Transactions on Mechatronics, 2006: 169-178.
- [21] Tan J., Xi N., Wang Y. Integrated Task Planning and Control for Mobile Manipulators. Proc. International Journal of Robotics Research, 2003: 337-354.
- [22] Roth B. "Advances in Robot Kinematics". Springer, Stanford University, U. S. A., 2006.
- [23] Goris K. Autonomous Mobile Robot Mechanical Design. Vrije Universiteit Brussel, Engineering Degree Thesis, Brussels, Belgium, 2005.
- [24] Dimitrios S. A. Analytical Configuration of Wheeled Robotic Locomotion. Carnegie Mellon University, Doctoral Thesis, U. S. A., 2001.
- [25] Zúñiga L. A., Pedraza J. C., Gorrostieta E., García L., Ramos J. M., Herrera R. Modeling and Simulation of a Mechatronic Unit EOD/IEDD. International

- Conference on Methods and Models in Automation and Robotics, 2009.
- [26] Fruchard M., Morin P., Samson C. A Framework for the Control of Nonholonomic Mobile Manipulators. *International Journal of Robotics Research*, 2006; 25(8): 745-780.
- [27] Mazur A., Szakiel D. On Path Following Control of Nonholonomic Mobile Manipulators. *Int. J. Appl. Math. Comput. Sci.* 2009; 19(4): 561-574.
- [28] Kelly, R., Santibáñez, V. *Control de Movimiento de Robots Manipuladores*. Editorial Prentice Hall, edición 2003; ISBN: 84-205-3831-0.
- [29] Zúñiga L. A., Pedraza J. C., Gorrostieta E., Ramos J. M. New approach to Modeling and Simulation Methodology for the Mechatronic Design of IEDD-Unmanned Wheeled Mobile Manipulator. *International Conference on Electronics, Robotics and Automotive Mechanics Conference, CERMA, México, D. F.*, 2010.
- [30] Zúñiga L. A., Skodny T., Pedraza J. C., Gorrostieta E. Systematic Analysis of an IEDD Unit based in a New Methodology for Modeling and Simulation. *Journal of Advanced Robotics, INTECH, Austria*, 2010; 7: 93-100.